applied sciences

MDPI

Article

Internal Observation Method of Temporary Structures Covered with a Construction Safety Net Using Image Processing and Unmanned Aerial Vehicles (UAVs)

Min-Guk Kang [1], Seung-Hyeon Shin [2], Hyeon-Ji Jeong [3] and Jeong-Hun Won [1,*]

[1] Department of Safety Engineering, Chungbuk National University, Cheongju 28644, Republic of Korea; 4266kmg@gmail.com
[2] Department of Big Data, Chungbuk National University, Cheongju 28644, Republic of Korea; shshin0317@chungbuk.ac.kr
[3] Department of Disaster Prevention Engineering, Chungbuk National University, Cheongju 28644, Republic of Korea; gus1895@naver.com
* Correspondence: jhwon@chungbuk.ac.kr

Abstract: This study proposes a method for observing the inside of a temporary structure covered with a construction safety net using an image processing technique and 3D modeling. Images of the temporary structures were obtained using unmanned aerial vehicles (UAVs). Observing the inside of temporary structures is limited to using UAVs due to construction safety nets that act as obstacles. To solve this problem, the histogram equalization and grayscale stretching techniques were used to visualize the inside of a temporary structure covered by safety nets. After verifying the proposed method with small scale specimens, the proposed method was applied to climbing formwork installed at a construction site. Three-dimensional modeling technique was combined with improved images that were processed using the proposed method. The results indicated that the proposed method could identify internal objects that were not visible owing to safety nets. By comparing the original and improved images obtained through applying the proposed method, four target objects located inside the climbing formwork that were not visible owing to safety nets were sufficiently identified in the improved images. Thus, the proposed method can be effectively applied to identify the internal objects of temporary structures covered with safety nets.

Keywords: temporary structure; construction safety net; image processing technique; 3D modeling; unmanned aerial vehicles (UAVs); internal observation

check for updates

Academic Editors: Fernanda Rodrigues, Joana Duarte and Antonio José Carpio de los Pinos

Received: 11 January 2025
Revised: 28 January 2025
Accepted: 30 January 2025
Published: 31 January 2025

Citation: Kang, M.-G.; Shin, S.-H.; Jeong, H.-J.; Won, J.-H. Internal Observation Method of Temporary Structures Covered with a Construction Safety Net Using Image Processing and Unmanned Aerial Vehicles (UAVs). *Appl. Sci.* **2025**, *15*, 1488. https://doi.org/10.3390/app15031488

Copyright: © 2025 by the authors. Licensee MDPI, Basel, Switzerland. This article is an open access article distributed under the terms and conditions of the Creative Commons Attribution (CC BY) license (https://creativecommons.org/licenses/by/4.0/).

1. Introduction

Various methods have been employed to prevent accidents at construction sites, among which, the use of unmanned aerial vehicles (UAVs) as safety management tools at construction sites is increasing [1,2]. One of the areas where UAVs are likely to be used at construction sites is for the safety management of temporary structures. During the construction process, it is important to check the structural defects of the temporary structure and the working conditions in the temporary structure, such as scaffolding, supports, and climbing formworks. Site managers apparently have trouble managing the installation condition of temporary structures and the unsafe behavior of workers, especially for large construction sites and high-rise buildings because access and movement are time-consuming. If UAVs can be used to inspect temporary structures attached to the exterior of buildings, site managers can efficiently manage the temporary structures.

However, when observing the inside of a temporary structure from the outside using UAVs, it is difficult to determine the accuracy of the installation condition of the structural members and the condition of workers wearing personal protective equipment, owing to the attachment of the construction safety net, which should be installed on the outer surface of the temporary structure in the form of a net and fixed to the temporary structure members to prevent workers from falling. Thus, the utilization of UAVs is limited because the safety net acts as an obstacle for viewing the internal object from the images obtained by UAVs. As far as the authors know, there is no method available to observe the inside of a temporary structure covered with a construction safety net. The only existing method is to visually observe the image of the temporary structure covered with the construction safety net, but the presence of the safety net makes it impossible to clearly observe the inside of the temporary structure. To solve this problem, a new approach based on an image processing technique that can reduce the blocking phenomenon of the construction safety net is necessary.

Various studies have been conducted on methods utilizing images obtained from UAVs, in particular in the fields of construction sites, military, disaster management, environmental monitoring, digital mapping, and orthographic image production [3–10]. The use of UAVs and 3D scanning is also increasing in the field of cultural heritage and archeology, where precise data and detailed work are required [11–13]. Specifically, an UAV image-based facility inspection method [14] was proposed as an alternative to the conventional visual inspection method to efficiently inspect aging facilities. In this method, a reference image database is built based on images captured using an UAV, and the newly acquired images are automatically processed to identify and check for the deformed parts on the target surface of the facility. The applicability of UAV imaging for surveying construction sites and confirming their compliance with installation standards for temporary structures to improve safety management at construction sites was also studied [15]. Owing to the advantages of UAV image acquisition, it is possible to quickly document the condition of a construction site and measure it without interfering with the work of field personnel.

UAV imaging enables the study of image segmentation, character/face recognition, and extraction of meaningful areas from images. These image processing techniques are widely used in the architecture, medicine, military, and meteorological fields [16,17]. Recently, to overcome the limitations of the existing contrast enhancement techniques, an image contrast enhancement technique based on a clustering method, such as histogram stretching and histogram equalization, was proposed [18] because image contrast enhancement plays an important role in image processing. The number of clusters in the histogram was determined by analyzing the histogram of the original image, and the K-means algorithm [19] was used as the clustering method. Histogram equalization and stretching were selectively applied by comparing the histogram cluster range and ratio of the number of pixels in the cluster to the clustered images.

A method to overcome the limitations of UAVs is to combine image processing and 3D modeling. Accurately identifying the safety status of temporary structures is limited owing to the low resolution of the images captured by UAVs of the entire building in one sheet [20]. Three-dimensional (3D) modeling can supplement the limits of the inspection area identified by a flat image. Image registration is a process that determines a corresponding relationship when there is a part in which the same object appears in different images. In the field of computer vision, it is easy to find a corresponding relationship if two given images are nearly identical. However, if various transformations are provided between the two images, it is difficult to find a corresponding relationship [21–23].

To solve this problem, we utilized a method for separating the ground and building areas via a planarity analysis using an UAV-based point cloud that can be generated at

a low cost and can automatically create a building model. This technique performs a planarity analysis using the generated point cloud, selecting a ground plane, removing the ground from the point cloud, and generating an orthographic projection image using the point cloud and original point cloud [24]. Using the orthographically projected image, building candidates were selected via the outline detection algorithm, and non-buildings were excluded from the candidates using the building conditions. Finally, a 3D building model was created by converting the selected building area into 3D ground coordinates and specifying the height value.

Considering research related to safety nets, most of the research regarding safety nets involves comparative studies of regulations related to safety nets [25,26]. Research on using UAVs to prevent safety accidents at construction sites is increasing, but most research areas are 3D modeling [27,28], safety inspections [29,30], and monitoring unsafe working conditions using deep learning [31,32]. Even in research on obstacles that make it difficult to apply UAVs to construction sites, there is little research that mentions problems caused by safety nets installed on temporary structures [33].

To the best of our knowledge, no research has been conducted regarding the internal observation methods for the construction of safety nets. This study contributes to the reduction in accidents at construction sites by proposing a technology that can observe the internal objects inside construction safety nets installed at construction sites. The purpose of this study was to propose an observation method that can identify the internal objects inside a temporary structure covered with a construction safety net using an image processing technique and 3D modeling. The proposed method can be helpful in inspecting temporary structures by observing changes in their installation status, dismantling of connections, and damage during various operations that occur after net installation. This is performed by comparing the image before installing a construction safety net and the image processed through the proposed method after safety net installation. When applying temporary structure safety inspection technology using AI, images taken before construction safety net installation can serve as a guide when observing image processed images after net installation.

2. Proposed Method

2.1. Temporary Structure Inside Observation Process

The proposed method, which can observe the internal objects inside a construction safety net, is shown in Figure 1. UAVs were used to capture pictures of a temporary structure with a target construction safety net installed, and image processing techniques were used for internal observations. Histogram equalization and grayscale stretching techniques were used for image processing, and 3D modeling was performed.

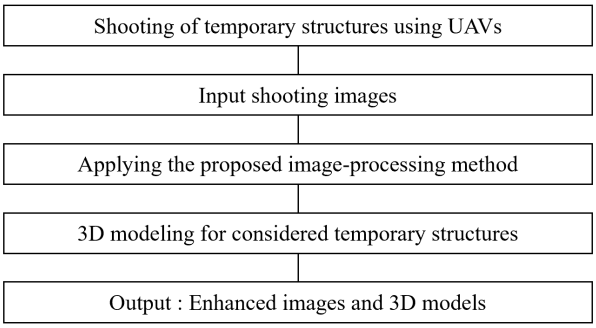


Figure 1. Proposed process for the internal observation of a temporary structure with safety nets.

2.2. Image Processing Method

The proposed image processing method is shown in Figure 2, which focuses on a combination of various image processing techniques to reduce blocking caused by construction safety nets. The main techniques used in the image processing sequence are histogram equalization and grayscale stretching, which are well-known image processing techniques [34,35].

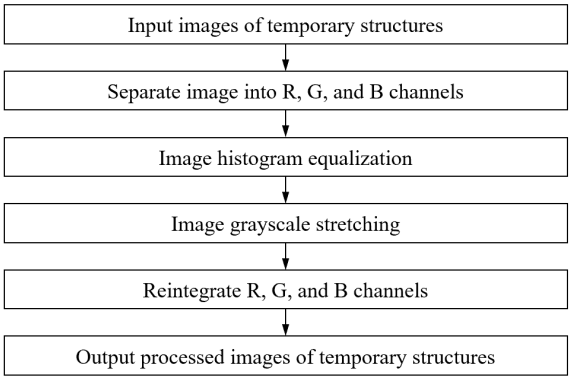


Figure 2. Proposed image processing sequence.

The original image was uploaded to the program developed in Step 1. In Step 2, the colored image in the uploaded file was converted to grayscale and separated into R, G, and B channels in grayscale units. In Step 3, the image histogram equalization technique was applied to the R, G, and B channels, which improved the resolution by equalizing the histogram shape deflected to one side. In Step 4, the image grayscale stretching technique was applied to the R, G, and B channels, which improved the contrast by converting images with pixel values ranging from 0 to 255 to "0" below the reference value, multiplied by a certain amount for the pixel value in the center, and "255" above the last reference value. The relationship between the output value and input value of the grayscale technique is as shown in Equation (1):

$$g(x,y) = \frac{f(x,y) - G_{min}}{G_{max} - G_{min}} \times 255, \quad (1)$$

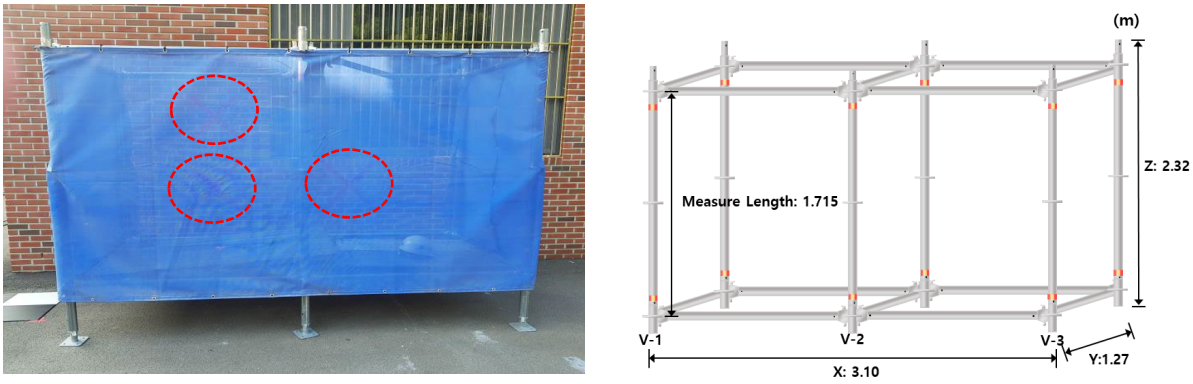
where $g(x,y)$ is the output value of grayscale technique and $f(x,y)$ is the input value. G_{min} and G_{max} are the lowest and largest grayscale values among the pixel values of the input image.

In this study, the input and output values were set as follows to improve image contrast. For the internal observation of the safety net, the input values were set to 0–64 and 191–255, and the output values were set to 0–95 and 190–204. In Step 5, the R, G, and B channels were integrated and converted into a 3D image, which produced an improved image in Step 6 (last step). The image processing technology used a MATLAB program to apply histogram equalization and grayscale stretching techniques, and controlled construction safety net from the images obtained.

3. Small Scale Experimental Test

3.1. Experimental Temporary Structure

The efficiency of the proposed method may vary depending on the color and denier value of the construction safety net. In this study, widely used construction safety nets in Korean construction sites were considered to test the feasibility of the proposed method. As the denier of the construction safety net most commonly used at Korean construction sites is 1500 denier, the temporary experimental structure was manufactured using a 1500-denier construction safety net (Figure 3a). A denier indicates the fiber density. Since colors such as blue, gray, red, and green are mainly used in construction safety nets, a blue safety net was considered in the small-scale experimental test.



(**a**) (**b**)

Figure 3. Temporary experimental structure: (**a**) Photo of temporary structure considered; (**b**) Length of temporary structure (unit: m).

The dimensions of the temporary structure were 3.10 × 1.27 × 2.32 m; the length of each end of the vertical member was measured to minimize the measurement error owing to the structural displacement during 3D modeling (Figure 3b). In addition, to check the effect of the image processing technique, three "X" shape marks were applied using red tape on the back wall of the temporary structure. The "X" markings in the red circle of the photo are vaguely demonstrated. In addition, a hard hat, tape measure, and hammer were randomly placed on the work platform to compare the difference between the original image and the image improved with the application or proposed method.

3.2. Image Shooting

When taking images of the target temporary experimental structure, weather conditions (e.g., rainy or snowy days) and positions (e.g., backlighting) are important factors because they affect the illuminance of the image. As the visibility of the processed image can be affected by the illuminance of the original image, the proposed method may be affected to some extent by the illuminance. As this study focused on verifying the feasibility of the proposed method, image shooting was conducted under good weather conditions and no backlight.

The used UAV is not an expensive piece of equipment considering its field applicability, and it is easily available. The temporary structures were photographed using the DJI Mini 2 model, which can determine its own position and stabilize itself by using a GPS and downward vision system. The specifications of the used UAV are listed in Table 1. The shooting path (Figure 4) was semicircular, at altitudes of 2 m and 4 m and angles of 30 °and 45°, respectively, to the ground centered on the specimen. A total of 100 images were obtained.

Table 1. Specifications of UAV (DJI Mini 2 model).

Category	Content	Category	Content
Camera sensor	1/1.2″ CMOS, Effective pixels: 12 m	Camera lens	Fov: 83° 35 mm format equivalent: 24 mm Aperture: f/2.8 Focus range: 1 m to ∞
Takeoff weight	249 g	Max ascent speed	2 m/s
Max speed	6 m/s	GNSS	GPS + GLONASS + ALILEO
Max flight time	31 min	Max descent speed	1.5 m/s

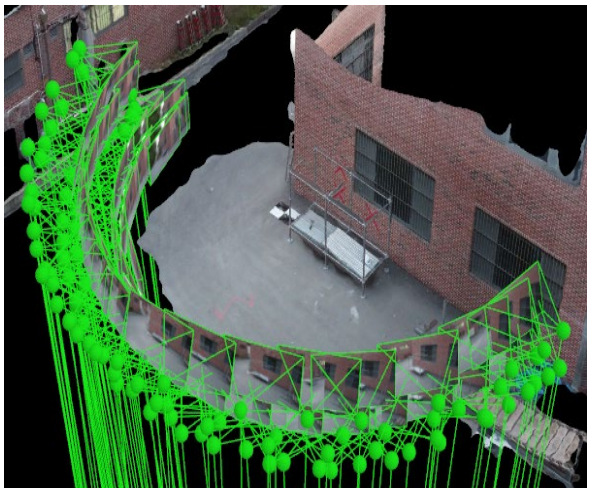


Figure 4. Image shooting path.

3.3. Comparison of Original Image and Improved Image

The original image was modified using the proposed image processing method. In Step 2, the original image was divided into R, G, and B channels after the colored image was converted to grayscale. Figure 5 confirms that the original image was biased towards a certain pixel value. In Step 3, the shape was deflected to one side (Figure 6) by applying the image histogram equalization technique to the R, G, and B channels. Figure 7 presents the results of the image grayscale stretching technique, which was applied to the R, G, and B channels in Step 4.

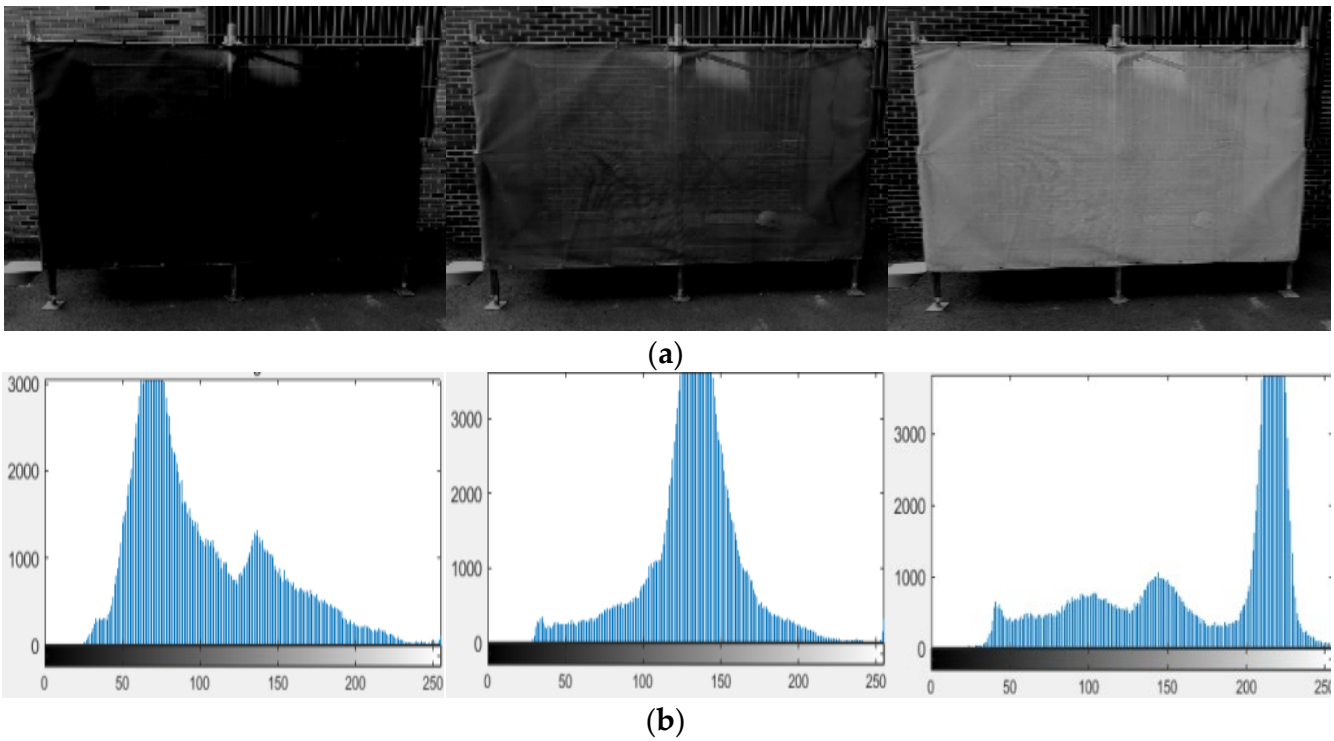


Figure 5. Results of the image separated into R, G, and B channels and the histogram in Step 2: (**a**) Red, green, and blue channels; (**b**) Histograms of red, green, and blue channels.

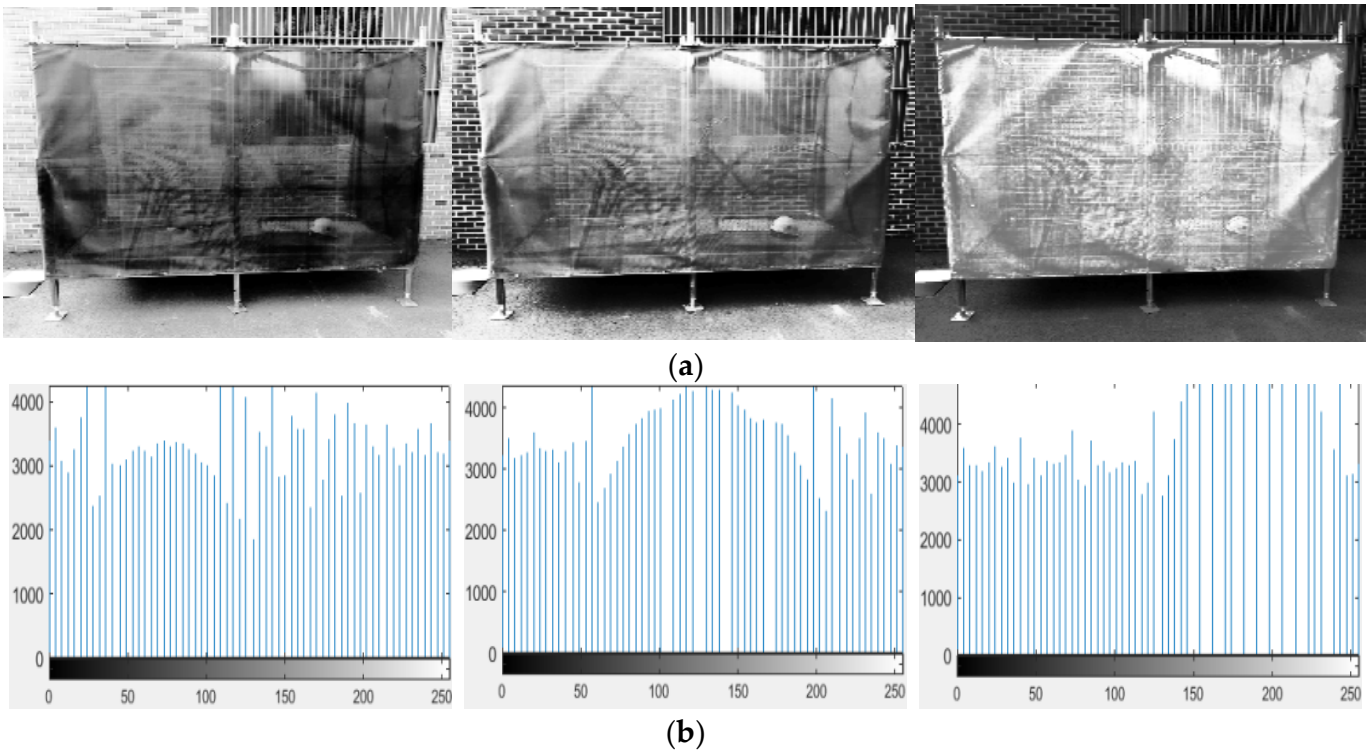


Figure 6. Results of the image separated into R, G, and B channels and the histogram in Step 3: (**a**) Red, green, and blue channels; (**b**) Histograms of red, green, and blue channels.

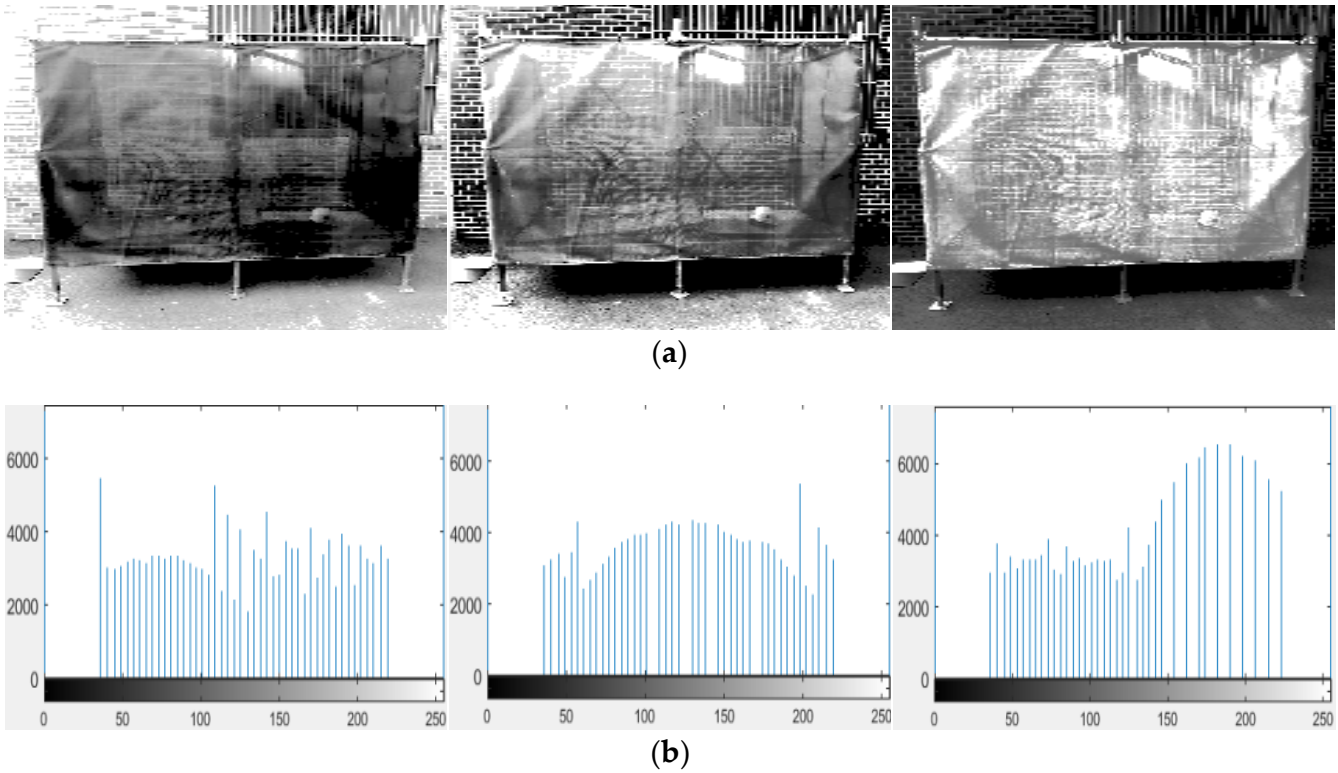
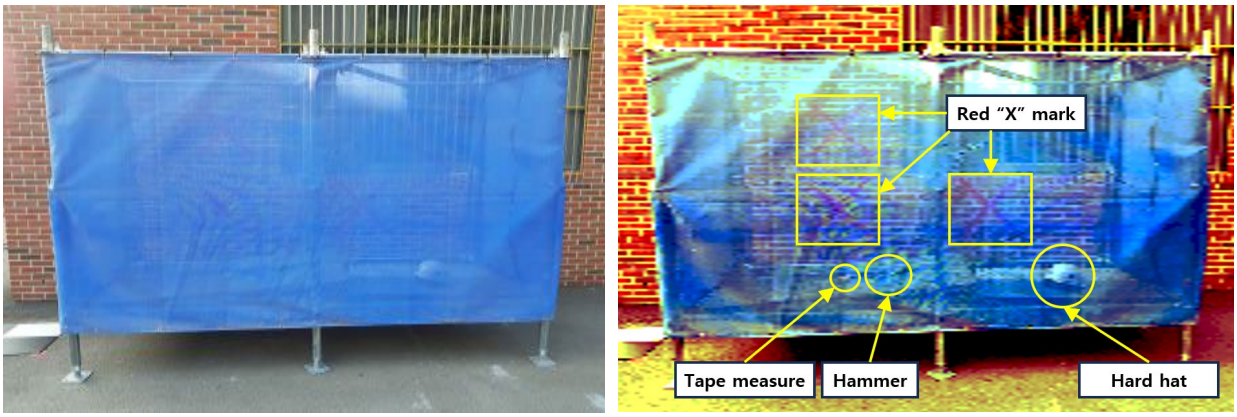


Figure 7. Results of the image separated into R, G, and B channels and the histogram in Step 4: (**a**) Red, green, and blue channels; (**b**) Histograms of red, green, and blue channels.

After Step 5, the improved image was presented by integrating the R, G, and B channels. Figure 8 shows a comparison of the original and improved images. The interior of the construction safety net in the original images prior to the application of image processing

cannot be sufficiently visualized, including the "X" mark and other objects placed on the work platform (Figure 8a). On the contrary, in the improved image with the implementation of the proposed method, the red "X" mark was clearly discerned. The overall identification of objects on the work platform apparently improved (Figure 8b). Considering the hard hat, the shape appeared to be more clearly identified, although it was also partially identified in the original image. The hammer that was not visible in the original image appeared somewhat identifiable in the improved image. The shape of the hammer was not clearly identifiable because the color of the working platform and body of the hammer were the same. The measuring tape was also approximately identifiable in the improved images.



(**a**) (**b**)

Figure 8. Comparison of the original and improved images: (**a**) Original image (Step 1); (**b**) Improved image (Step 6).

3.4. Three-Dimensional Modeling

The image taken as a single photo of the temporary structure using UAVs has low resolution, so it is difficult to accurately inspect the status of the temporary structure. To solve this problem, the temporary structure was photographed from various sides and angles and 3D modeling was applied. Three-dimensional modeling naturally connects the entire shooting area as a single image based on the characteristics of the overlapping areas to overcome the limitations of cameras with a narrow view as well as the contrast of the area photographed. The point-cloud transformation of a two-dimensional image captured by the UAV is a set of identifiable reference points in the captured image. Point cloud-based 3D data conversion is a 3D mesh construction process that expresses point cloud data in 3D using triangles of various sizes.

For 3D modeling, the Pix4D mapper program was used, which is an image processing software based on a technique for automatically finding common points between images of the target structures. The features of this program include the identification of a number of feature points in an image and their connection between images. In this study, after performing image processing on the 2D images acquired by an UAV, 3D modeling is carried out in the following steps: initial matching of images (step 1); point cloud and mesh generation (step 2); Digital Surface Model (DSM) Digital Terrain Model (DTM), Digital Elevation Model (DEM), and orthoimage creation (step 3). The 3D modeling process is shown in Figure 9. Figure 10 presents the results of steps 1 and 2, which include the shooting angle of the UAVs, point cloud of the experimental temporary structures, and triangular mesh for considered temporary structure. A ground control point (GCP) survey was conducted to convert the coordinate values of the captured images into ground coordinates. Three GCPs representing the highest resolution and positioning accuracy were set.

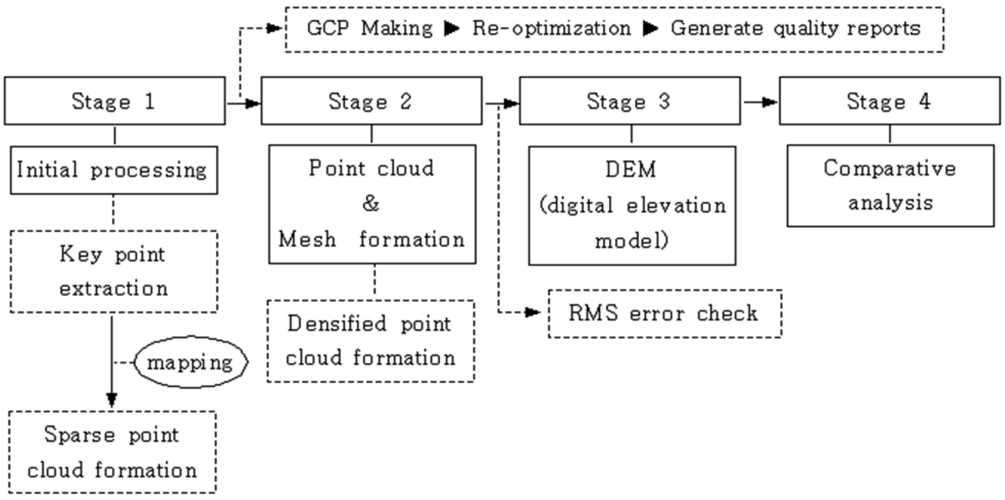


Figure 9. Three-dimensional modeling process.



(**a**) (**b**) (**c**)

Figure 10. Three-dimensional modeling: (**a**) Shooting angle; (**c**) Point cloud creation; (**c**) Triangular mesh creation.

Image distortion must be taken into consideration in 3D modeling using an UAV. The main causes of image distortion in 3D modeling include errors in the shooting process (flight path, camera angle, lack of overlap) and the image processing process (alignment errors, lack of feature points). In order to mitigate distortion, the planned flight path was maintained when shooting with an UAV and data density was increased by securing 70–90% overlap and shooting at various altitudes. Additional methods to reduce distortion include improving camera image quality and adding GCP to improve location accuracy.

To quantitatively evaluate the 3D modeling results, GSD (Ground Sampling Distance) and RMSE (Root Mean Square Error) were evaluated. GSD refers to the distance that one pixel occupies on the ground. The smaller the value, the higher the resolution, and the more precise the 3D model is created. RMSE represents the average error between predicted coordinates and actual coordinates, and the smaller the value, the more consistent it is with the actual structure. The following represent the GSD and RMSE evaluation equations.

$$GSD = \frac{H \times S}{F}, \tag{2}$$

$$RMSE = \frac{1}{n}\sqrt{\sum_{i=1}^{n}\left(X_i - X_i'\right)^2 + \left(Y_i - Y_i'\right)^2 + \left(Z_i - Z_i'\right)^2}, \tag{3}$$

where H is the UAV's flight altitude (m), S is the pixel size of the sensor (mm), and F is the focal length of the lens. X, Y, Z are the actual coordinates and X′, Y′, Z′ are the coordinates

predicted by the model. n is the number of data points. The GSD and RMSE evaluation results for 3D modeling of the considered experimental temporary structure are shown in Table 2.

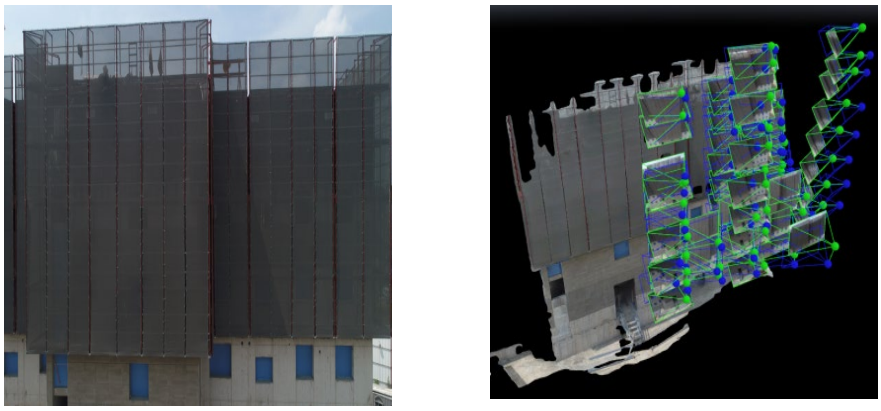
Table 2. Quantitative evaluation metrics of 3D modeling quality.

Category	GSD (cm/pixel)	RMSE (cm)
Value	0.49	1.3

4. Field Experiment

4.1. Temporary Structure

The temporary experimental structures used to verify the proposed method are limited in size and are typically smaller than the actual temporary structures installed at construction sites. An onsite test was conducted to investigate the effectiveness and feasibility of the proposed method. The temporary structure considered was a climbing formwork (crane-climbing type) covered with a construction safety net that was used to build the apartment (Figure 11a). The color of the construction safety net installed on the climbing formwork is gray, and the denier value is 1500.



(**a**) (**b**)

Figure 11. The climbing formwork and shooting points are considered: (**a**) Photo of considered climbing formwork; (**b**) Shooting point.

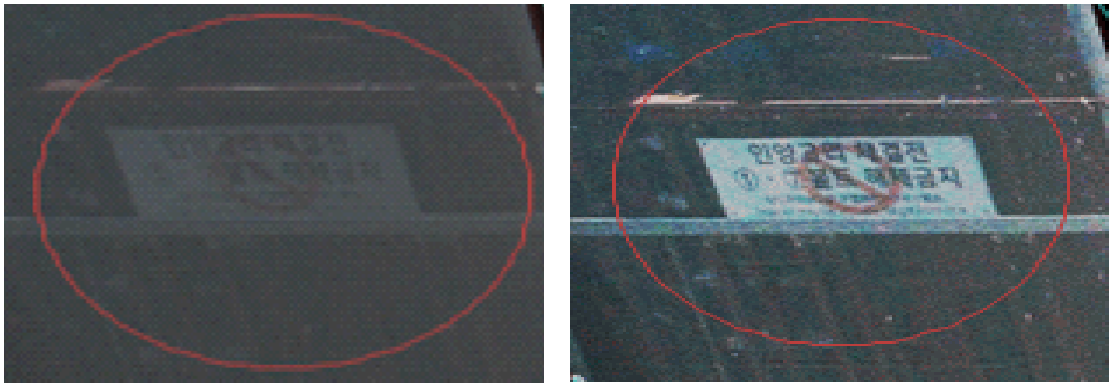
For the 3D modeling, 100 images were captured using an UAV. To achieve high-quality 3D modeling, each photograph was acquired at 30° and 45° downward angle relative to the front of the UAV, ensuring an overlap rate of more than 90% in the vertical direction and 80% or more in the horizontal direction (Figure 11b). Image shooting of the climbing formwork was conducted in clear weather conditions. In the case of backlighting conditions, image shooting was conducted with a certain amount of backlighting occurring.

4.2. Verification of Proposed Image Processing Method

To validate the applicability and effectiveness of the proposed method, target objects inside the climbing formwork covered with a safety net were selected. The four objects were safety signs, personal protective equipment worn by workers, climbing formwork ladders, and work platforms, which are essential equipment to ensure the safety of workers.

Regarding identification of the safety signs, the original and improved images were compared, as shown in Figure 12. The Korean text on the safety signs was regarding the dismantling of the bolt of the climbing formwork. A typical accident that occurs in climbing formworks is when workers arbitrarily disassemble the connection bolt before the lifting hook is fastened to the climbing formwork, causing the workers to fall. The red circle mark shown in Figure 12 indicates that the dismantling of connection bolts ① and ⑦

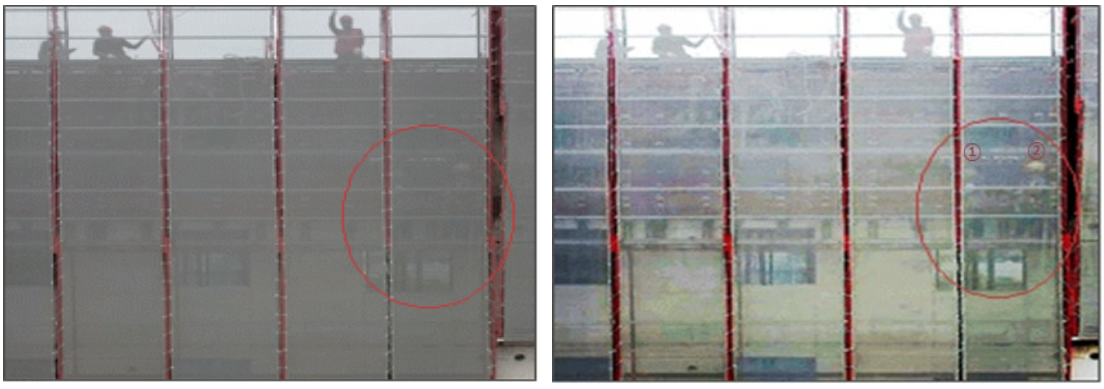
is prohibited before fastening the lifting hook to the climbing formwork. In the original image, it was difficult to recognize the attachment state of the safety sign and text owing to the construction safety net (Figure 12a). However, the application of the proposed image processing technology leads to an enhancement in the image contrast, thereby improving the visibility of the installation status of safety signs, ultimately achieving observable levels (Figure 12b). Using the proposed image processing method, the installation state and contents of the safety signs can be clearly observed.



(**a**) (**b**)

Figure 12. Identification of the attachment state and content of the safety sign; (**a**) Original image; (**b**) After improvement.

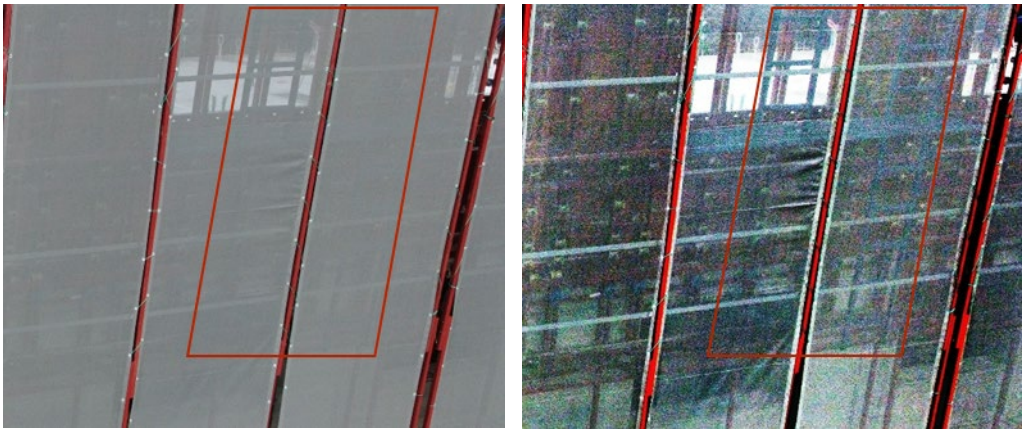
Workers must wear hard hats as personal protective equipment (PPE) during construction work to ensure safety in the event of an accident. At construction sites, managers, including those who are responsible for safety, should ensure that workers wear hard hats. Monitoring all areas of large construction sites is difficult because certain workers work without PPE, such as hard hats. In particular, it is challenging to monitor whether PPE is worn by workers on climbing formworks using UAVs, primarily owing to the presence of construction safety nets. It is difficult to determine the number of workers wearing hard hats, as shown by the red circle in Figure 13a. However, in the image improved by the proposed image processing method, the identification of internal work was enhanced. As shown in Figure 13b, it is evident that the two workers were wearing yellow hard hats. Using the proposed method combined with UAVs, construction managers do not need to directly access the climbing formwork to inspect the compliance of workers with safety and protective equipment. A more effective means of safety management is anticipated because the workers can be easily monitored from outside the climbing formwork.



(**a**) (**b**)

Figure 13. Inspection of workers wearing hard hats: (**a**) Original image; (**b**) After improvement.

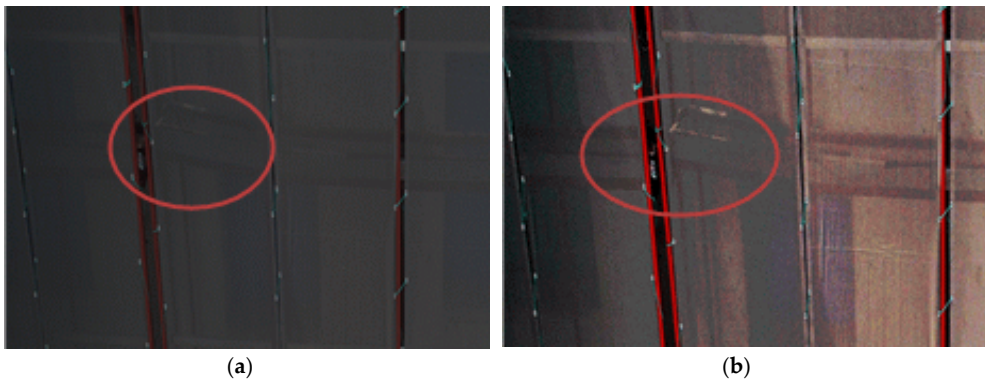
According to regulations, a ladder should be installed on the climbing formwork to facilitate the movement of workers between floors. However, its usability may be compromised owing to inadequate installation conditions, such as poor installation quality and failure to adhere to proper installation intervals. The installation status of the ladders is challenging to observe, despite using UAVs to capture the footage outside the climbing formwork, as indicated by the red square box (Figure 14a). However, when the proposed image processing technology was utilized, installation of the two blue ladders connecting the layers of the climbing formwork became evident (Figure 14b). The proposed image processing method is expected to enhance the effective management of ladder installations on the climbing formworks by externally enabling the observation of ladder installation defects using UAVs.



(**a**) (**b**)

Figure 14. Installation status of climbing formwork ladder: (**a**) Original image; (**b**) After improvement.

A work platform should be placed in the climbing formwork to guarantee the safety and movement of workers. It should be correctly installed without bending or deformation in accordance with the regulations. Moreover, the incorrect installation of a work platform can potentially lead to accidents, including falls or tripping incidents, when workers navigate the platform. When inspecting a work platform in a climbing formwork using UAVs, it is difficult to observe whether it is properly installed according to regulations owing to the construction safety net (Figure 15a). When the proposed image processing was applied to the original image, the work platform in the region delineated by a red circle was apparently inadequately installed (Figure 15b). Therefore, the proposed image processing method can easily be employed for safety management by observing the installation state of a climbing formwork plate from an external view.



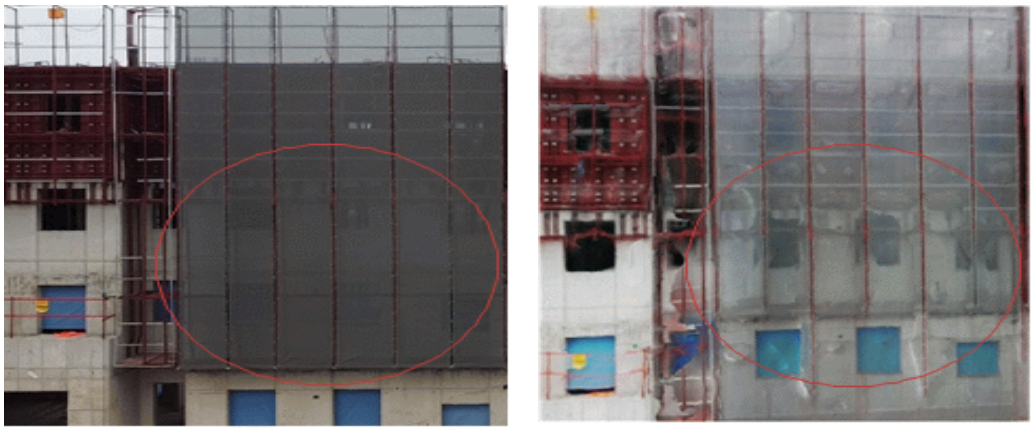
(**a**) (**b**)

Figure 15. Installation status of work platforms: (**a**) Original image; (**b**) After improvement.

4.3. Results of 3D Modeling Utilizing the Proposed Internal Observation Method

Safety management at construction sites can be vulnerable to accidents owing to the extensive deployment of personnel engaged in a variety of tasks over a large area. Site safety management faces limitations owing to the shortage of personnel to oversee expansive areas. Therefore, utilizing 3D models of construction sites is effective for simplifying the observation of spaces within the construction safety net that are typically difficult for safety managers to access and monitor. The 3D model was developed using improved images to aid safety management.

Because the original image was 2D, only one side of the climbing formwork was observable, and the internal examination was hindered, owing to the presence of the construction safety net (Figure 16a). The image processing method was applied to 100 original images to enable the identification of internal objects, and these were combined via 3D modeling. The internal components of the climbing formwork, known for their limited accessibility and observation by safety managers, became visible from various perspectives through the application of 3D modeling (Figure 16b). It can be clearly confirmed that the inside of the climbing formwork, which could not be seen in the original image due to the safety net, could be observed through a 3D model using the improved image by the image processing method. Therefore, it can be seen that the proposed method is effective. It is noted that certain distortions were encountered during the 3D modeling process, which were attributed to insufficient image information for accurately matching the corresponding areas in the 3D model. This issue can be resolved by utilizing UAVs equipped with high-quality cameras or improving location accuracy by adding GCP.



(**a**) (**b**)

Figure 16. Comparison of experimental images and 3D modeling results after image processing: (**a**) Experimental image; (**b**) 3D modeling after image processing.

4.4. Quantitative Validation of the Proposed Image Processing Method

The proposed image processing method was quantitatively validated using Peak Signal-to-Noise Ratio (PSNR) and Structural Similarity Index Measure (SSIM) in Google Colab [36]. PSNR is a metric used to measure the quality of an image compared to an original image. It is expressed in decibels (dB) and calculated using the Mean Squared Error (MSE) between the original and processed images. MSE measures the mean square differences between corresponding pixel values of the original image I and the processed image K (image size m × n). MSE and PSNR are as follows:

$$MSE = \frac{1}{mn} = \sum_{i=0}^{m-1} \sum_{j=0}^{n-1} \left[I(i,j) - K(i,j) \right]^2, \quad (4)$$

$$PSNR = 10\log_{10}\left(\frac{{MAX_I}^2}{MSE}\right), \quad (5)$$

where MAX_I is the maximum possible pixel value of the image, such as 255 in 8-bit grayscale image.

A higher PSNR value generally indicates less distortion and therefore generally better image quality. SSIM is designed to evaluate the perceptual similarity between two images by considering luminance, contrast, and structural similarities. Unlike PSNR, which measures absolute errors, SSIM evaluates how similar the processed image is to the reference image from a human visual perspective.

$$SSIM(x,y) = \frac{\left({\mu_x}^2 + {\mu_y}^2 + C_1\right)}{\left({\sigma_x}^2 + {\sigma_y}^2 + C_2\right)\left(2\mu_x\mu_y + C_1\right)\left(2\sigma_{xy} + C_2\right)}, \quad (6)$$

where μ_x and μ_y are the mean intensities of images x and y. σ_x^2 and σ_y^2 are the variances of images x and y. σ_{xy} is the covariance between the two images. C_1 and C_2 are small constants to prevent division by zero. The SSIM value ranges from -1 to 1, with 1 indicating perfect similarity, 0 suggesting no similarity, and negative value implying structural dissimilarity.

Table 3 shows the PSNR and SSIM measurements for the images to which the proposed method in Figures 11–15 was applied. Figure 11 shows the highest PSNR, followed by Figure 14. In the case of SSIM, it was evaluated to be the highest in Figure 14.

Table 3. Comparison of quantitative values of image processing performance using PSNR and SSIM.

Values	Figure 11	Figure 12	Figure 13	Figure 14	Figure 15
PSNR (dB)	29.46 dB	27.90 dB	27.85 dB	28.04 dB	27.84 dB
SSIM	0.0423	0.2808	0.1715	0.3119	0.2732

In this study, the entry-level UAV models with low price were used to verify the proposed method. A camera resolution, sensor quality, GPS, and IMU are the main items that determine the price of the UAV. High-level UAV models provide high resolution, distortion correction functions, and stable aircraft flight capabilities, so more accurate images can be obtained through the use of high-level UAVs. Although it is difficult to generalize the performance shown in entry-level UAVs to other UAVs, it can be expected that better results can be obtained if a high-level UAV is used.

5. Conclusions

This study proposes a method for observing the inside of a temporary structure with a construction safety net using image processing, unmanned aerial vehicles (UAVs), and 3D modeling. The applicability and effectiveness of the proposed method were verified by experimentally testing a small-scale temporary structure covered with a safety net and a field test for a climbing formwork; the following conclusions were drawn.

Two image processing techniques, including the histogram equalization and grayscale stretching techniques, were applied to observe the internal objects in temporary structures covered with construction safety nets, to ensure the safety of workers and prevent falling from significant heights. The installed construction safety net was composed of a single material, and when the captured image was analyzed, it was composed of a certain pixel value. The pixel values constituting the image of the construction safety net were believed to be biased, and the resolution was improved by equalizing this bias. A grayscale stretching technique was applied to prevent excessive equalization, which is a disadvantage of this technique. Moreover, 3D modeling can be used to observe a wide area from various angles.

Therefore, the possibility of using it to check the structural deformation of a temporary structure was identified.

The applicability of the internal observation technology for a temporary structure at a construction site was estimated by selecting a target object in a climbing formwork that was temporarily installed and used at a high-rise building construction site. The improved images obtained by the proposed method clearly identified the four test objects (safety signs, PPE, etc.) whereas the original image did not. Therefore, implementing the proposed technology in temporary structures with construction safety nets can help prevent safety incidents for workers operating in areas that pose challenges to safety managers in terms of accessibility and oversight.

The efficiency of the proposed method may vary depending on the colors, materials, and denier values. The limitation of this study is that the colors of the applied construction safety net are blue and gray, and only one denier value was applied. This limitation makes it difficult to expect consistent performance depending on the field conditions. However, this study verified the possibility of observing the internal objects of a temporary structure covered with a safety net at a construction site using an UAV. Future research will be performed on various variables of construction safety nets, such as the color and denier values. Additionally, research will be conducted to evaluate the impact of external factors such as weather, illumination, backlighting, and the hardware capacity of UAVs on the performance of the proposed method.

Author Contributions: Conceptualization, M.-G.K. and J.-H.W.; methodology, M.-G.K.; software, M.-G.K. and H.-J.J.; validation, M.-G.K., S.-H.S. and H.-J.J.; formal analysis, M.-G.K.; investigation, S.-H.S.; writing—original draft preparation, M.-G.K.; writing—review and editing, J.-H.W.; visualization, S.-H.S.; supervision, J.-H.W. All authors have read and agreed to the published version of the manuscript.

Funding: This research was supported by the "Leaders in Industry-University Cooperation 3.0" Project, funded by the Ministry of Education and National Research Foundation of Korea. This research was partially supported by Basic Science Research Program through the National Research Foundation of Korea (NRF) funded by the Ministry of Education (No. RS-2024-00407154). It also was partially supported by the Human Resources Development of the Korea Insitute of Energy Technology Evaluation and Planning (KETEP) grant funded by the Korea government (No. 20224000000070).

Data Availability Statement: The raw data supporting the conclusions of this article will be made available by the authors on request.

Conflicts of Interest: The authors declare no conflicts of interest.

References

1. Mascarenas, D.; Flynn, E.; Todd, M.; Park, G.; Farrar, C. Wireless sensor technologies for monitoring civil structures. *J. Sound Vib.* **2008**, *42*, 16–21.
2. Jeong, E.; Seo, J.; Wacker, J.P. UAV-aided bridge inspection protocol through machine learning with improved visibility images. *Expert Syst. Appl.* **2022**, *197*, 116791. [CrossRef]
3. Yoo, H.-W.; Park, H.-S.; Jang, D.-S. Expert system for color image retrieval. *Expert Syst. Appl.* **2005**, *28*, 347–357. [CrossRef]
4. Butkiewicz, T.; Chang, R.; Wartell, Z.; Ribarsky, W. Visual Analysis for Live LIDAR Battlefield Change Detection. In Proceedings of the Defense and Security 2008: Special Sessions on Food Safety, Visual Analytics, Resource Restricted Embedded and Sensor Networks, and 3D Imaging and Display, Orlando, FL, USA, 15 April 2008; Volume 6983, pp. 69–78. [CrossRef]
5. Comert, R.; Kaplan, O. Object Based Building Extraction and Building Period Estimation from Unmanned Aerial Vehicle Data. In Proceedings of the ISPRS Annals of the Photogrammetry Remote Sensing and Spatial Information Sciences, Beijing, China, 7–10 May 2018; Volume 4, pp. 71–76. [CrossRef]
6. Koch, C.; Paal, S.G.; Rashidi, A.; Zhu, Z.; König, M.; Brilakis, I. Achievements and challenges in machine vision-based inspection of large concrete structures. *Adv. Struc. Eng.* **2014**, *17*, 303–318. [CrossRef]

7. Lins, R.G.; Givigi, S.N. Automatic crack detection and measurement based on image analysis. *IEEE Trans. Instrum. Meas.* **2016**, *65*, 583–590. [CrossRef]
8. Liu, P.; Chen, A.Y.; Huang, Y.N.; Han, J.Y.; Lai, J.S.; Kang, S.C.; Tsai, M.H. A review of rotorcraft unmanned aerial vehicle (UAV) developments and applications in civil engineering. *Smart Struct. Syst.* **2014**, *13*, 1065–1094. [CrossRef]
9. Martinez, J.G.; Gheisari, M.; Alarcón, L.F. UAV integration in current construction safety planning and monitoring processes: Case study of a high-rise building construction project in Chile. *J. Manag. Eng.* **2020**, *36*, 05020005. [CrossRef]
10. Rudol, P.; Doherty, P. Human Body Detection and Geolocalization for UAV Search and Rescue Missions Using Color and Thermal Imagery. In Proceedings of the 2008 IEEE Aerospace Conference, Big Sky, MT, USA, 1–8 March 2008. [CrossRef]
11. Pepe, M.; Alfio, V.S.; Costantino, D. UAV platforms and the SfM-MVS approach in the 3D surveys and modelling: A review in the cultural heritage field. *Appl. Sci.* **2022**, *12*, 12886. [CrossRef]
12. Themistocleous, K. The Use of UAVs for Cultural Heritage and Archaeology. In *Remote Sensing for Archaeology and Cultural Landscapes*; Springer: Cham, Switzerland, 2020; pp. 241–269. [CrossRef]
13. Kantaros, A.; Ganetsos, T.; Petrescu, F.I.T. Three-dimensional printing and 3D scanning: Emerging technologies exhibiting high potential in the field of cultural heritage. *Appl. Sci.* **2023**, *13*, 4777. [CrossRef]
14. Moore, J.; Tadinada, H.; Kirsche, K.; Perry, J.; Remen, F.; Tse, Z.T.H. Facility inspection using UAVs: A case study in the University of Georgia campus. *Int. J. Remote Sens.* **2018**, *39*, 7189–7200. [CrossRef]
15. Jeelani, I.; Gheisari, M. Safety challenges of UAV integration in construction: Conceptual analysis and future research roadmap. *Saf. Sci.* **2021**, *144*, 105473. [CrossRef]
16. Zhu, Z.; Brilakis, I. Concrete column recognition in images and videos. *J. Comput. Civil Eng.* **2010**, *24*, 478–487. [CrossRef]
17. Neto, J.; Arditi, D.; Evens, M. Using colors to detect structural components in digital pictures. *Comput. Aided Civil Infrastruct. Eng.* **2002**, *17*, 61–76. [CrossRef]
18. Abdullah-Al-Wadud, M.; Kabir, M.H.; Dewan, M.A.A.; Chae, O. A dynamic histogram equalization for image contrast enhancement. *IEEE Trans. Consum. Electron.* **2007**, *53*, 593–600. [CrossRef]
19. Ahmed, M.; Seraj, R.; Islam, S.M.S. The k-means algorithm: A comprehensive survey and performance evaluation. *Electron.* **2020**, *9*, 1295. [CrossRef]
20. Sansoni, G.; Trebeschi, M.; Docchio, F. State-of-the-art and applications of 3D imaging sensors in industry. cultural heritage, medicine, and criminal investigation. *Sensors* **2009**, *9*, 568–601. [CrossRef]
21. Alvarez, L.; Baumela, L.; Henriquez, P.; Marquez-Neila, P. Morphological Snakes. In Proceedings of the 2010 IEEE Computer Society Conference on Computer Vision and Pattern Recognition, San Franciso, CA, USA, 13–18 June 2010; pp. 2197–2202. [CrossRef]
22. Remondino, F.; Spera, M.G.; Nocerino, E.; Menna, F.; Nex, F.; Gonizzi-Barsanti, S. Dense image matching: Comparisons and analyses. In Proceedings of the Digital Heritage International Congress, Marseille, France, 28 October 2013; pp. 47–54. [CrossRef]
23. Snavely, N.; Seitz, S.M.; Szeliski, R. Modeling the world from internet photo collections. *Int. J. Comput. Vis.* **2008**, *80*, 189–210. [CrossRef]
24. Malihi, S.; Valadan Zoej, M.J.; Hahn, M.; Mokhtarzade, M.; Arefi, H. 3D Building Reconstruction Using Dense Photogrammetric Point Cloud. In Proceedings of the International Archives of the Photogrammetry, Remote Sensing and Spatial Information Sciences, Prague, Czech Republic, 12–19 July 2016; pp. 71–74. [CrossRef]
25. Filho, M.C.A.; Serra, S.M.B. Comparison between collective protective systems in Brazil: Safety platforms and safety net type V. *SN Appl. Sci.* **2020**, *2*, 2153. [CrossRef]
26. Çelik, G.T.; Aydınlı, S.; Bazaati, S. Safety net applications in developing countries: Turkey and Iran case study. *J. Constr. Eng. Manag. Innov.* **2021**, *4*, 12–21. [CrossRef]
27. Wang, C.; Tang, Y.; Kassem, M.A.; Chen, Z. UAV application for typhoon damage assessment in construction sites. *Appl. Sci.* **2022**, *12*, 6293. [CrossRef]
28. Kim, H.-J.; Kim, J.-Y.; Aim, J.-W.; Kim, S.-K.; Na, W.S. Unmanned aerial vehicle-based automated path generation of rollers for smart construction. *Electronics* **2024**, *13*, 138. [CrossRef]
29. Halder, S.; Afsari, K. Robots in inspection and monitoring of buildings and infrastructure: A systematic review. *Appl. Sci.* **2023**, *13*, 2304. [CrossRef]
30. Jiao, X.; Wu, N.; Zhang, X.; Fan, J.; Cai, Z.; Wang, Y.; Zhou, Z. Enhancing tower crane safety: A UAV-based intelligent inspection approach. *Buildings* **2024**, *14*, 1420. [CrossRef]
31. Liang, H.; Seo, S. UAV low-altitude remote sensing inspection system using a small target detection network for helmet wear detection. *Remote Sens.* **2023**, *15*, 196. [CrossRef]
32. Kumar, S.; Poyyamozhi, M.; Murugesan, B.; Rajamanickam, N.; Alroobaea, R.; Nureldeen, W. Investigation of unsafe construction site conditions using deep learning algorithms using unmanned aerial vehicles. *Sensors* **2024**, *24*, 6737. [CrossRef]
33. Akinradewo, O.; Aigbavboa, C.; Emere, C.; Ebiloma, D.O.; Akinshipe, O.; Oke, A. Barriers to the adoption of unmanned aerial vehicles for construction projects in South Africa. *Eng. Proc.* **2024**, *76*, 12. [CrossRef]

34. Gonzales, R.C.; Woods, R.E. *Digital Image Processing*, 4th ed.; Pearson: New York, NY, USA, 2018; pp. 133–152.
35. Helen, H. Image registration in medical applications. *J. Int. Soc. Simul. Surg.* **2014**, *1*, 62–66. [CrossRef]
36. Hore, A.; Ziou, D. Image Quality Metrics: PSNR vs SSIM. In Proceedings of the 2010 20th International Conference on Pattern Recognition, Istanbul, Türkiye, 23–26 August 2010; Volume 1, pp. 2366–2369. [CrossRef]

Disclaimer/Publisher's Note: The statements, opinions and data contained in all publications are solely those of the individual author(s) and contributor(s) and not of MDPI and/or the editor(s). MDPI and/or the editor(s) disclaim responsibility for any injury to people or property resulting from any ideas, methods, instructions or products referred to in the content.